Charge sensing of excited states in an isolated double quantum dot

A. C. Johnson and C. M. Marcus
Department of Physics, Harvard University, Cambridge, Massachusetts 02138, USA

M. P. Hanson and A. C. Gossard
Department of Materials, University of California, Santa Barbara, California 93106, USA
(Received 11 November 2004; published 31 March 2005)

Pulsed electrostatic gating combined with capacitive charge sensing is used to perform excited-state spectroscopy of an electrically isolated double-quantum-dot system. The tunneling rate of a single charge moving between the two dots is affected by the alignment of quantized energy levels; measured tunneling probabilities thereby reveal spectral features. Two pulse sequences are investigated, one of which, termed latched detection, allows measurement of a single tunneling event without repetition. Both provide excited-state spectroscopy without electrical contact to the double-dot system.

DOI: 10.1103/PhysRevB.71.115333 PACS number(s): 73.21.La, 73.23.Hk

Electrically controllable discrete quantum states found in quantum dot systems are efficient laboratories for the study of quantum coherence,[1] as well as a potential basis for quantum computation.[2] Measuring the spectrum and dynamics of quantum dots requires coupling to a macroscopic measurement apparatus, which in turn may act to reduce coherence.[3] Excited-state spectroscopy of single[4] and double[5,6] quantum dots has typically been performed using nonlinear transport, requiring tunnel coupling of the device to electron reservoirs.[6] This coupling perturbs the quantum states and may increase decoherence and heat the device, particularly at the large biases needed for spectroscopy far from the Fermi surface.

An alternative approach that we investigate in this article is to use capacitive charge sensing[7,8] combined with pulsed gate voltages that provide an excitation window.[9] Charge sensing has recently been used to probe excited-state spectra in a few-electron quantum dot coupled to one reservoir.[10] We investigate pulse-sense spectroscopy in an electrically isolated double quantum dot, where a *single charge*, moving between the two dots, is used to probe excited states. Local charge sensing by a quantum point contact (QPC) near one of the dots provides readout.

The pulse-sense method operates as follows. A *reset pulse* on two gates simultaneously opens the coupling between the dots and "tilts" the potential, putting the excess charge on a selected dot [the device is shown in Fig. 1(a)]. When the pulse is removed, each dot separately is in its ground state, but the double-dot system is out of equilibrium. The excess charge is given a finite time to tunnel to the other dot (the *probe* time). The probability of tunneling depends sensitively on the alignment of ground- and excited-state levels in the two dots. Whether or not the charge tunnels during the probe time is detected by a QPC sensor.

Two gate sequences are investigated. In the first, a short reset pulse is followed by a relatively long probe interval during which a low tunneling rate gives a moderate total probability for tunneling. By cycling the reset and probe steps, the QPC measures the average charge configuration, dominated by the probe step. This allows fine energy resolution, as the probe process is insensitive to both thermal effects and experimental difficulties associated with short pulses. The second sequence uses two pulses: the first resets the system; the second allows weak tunneling between dots. The second pulse is followed by an arbitrarily long interval

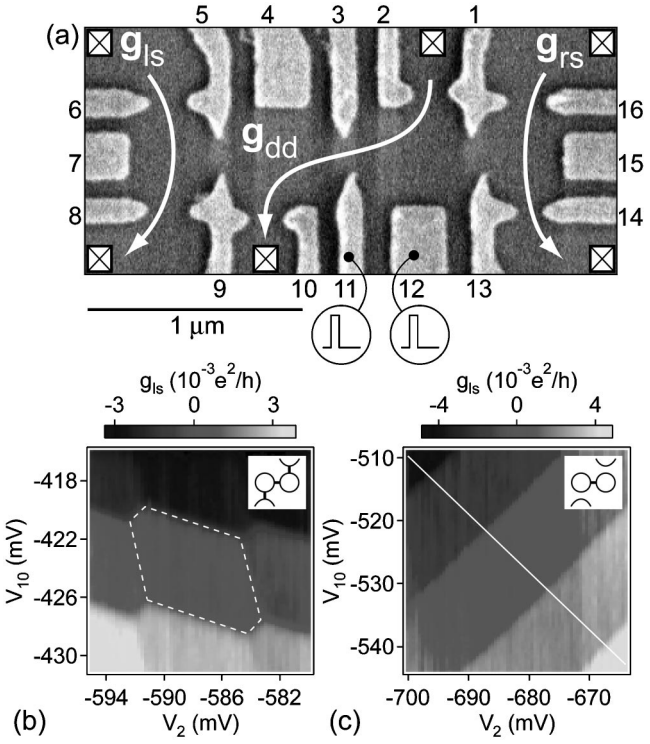

FIG. 1. (a) Scanning electron micrograph of a device identical in design to the one measured, consisting of a double quantum dot with a charge sensor on either side. High-bandwidth coaxial lines are attached to gates 11 and 12, dc lines to the other gates. (b) Left sensor signal as a function of gate voltages V_2 and V_{10} reveals hexagonal charge stability regions (one outlined with dashed lines) when the double dot is tunnel-coupled to leads. (c) Sensor signal with the double dot isolated from the leads. Only interdot transitions remain. In all pulse-sense experiments presented, the double dot is isolated (as in c) and V_2 and V_{10} are swept along a diagonal crossing these transitions (solid white line). A plane is subtracted in (b) and (c) to compensate direct coupling of gates 2 and 10 to the sensor.

(microseconds to hours, in principle) with the interdot barrier closed, so that each dot is completely isolated, with fixed charge. This sequence we term *latched detection*, because the measurement occurs after the double dot is latched into a final state, separating in time the charge dynamics and the measurement. If needed, the measurement could be turned off during the probe pulse, though here we make the measurement time much longer than the probe time and measure weakly, so that the total back action of the measurement on the system during the probe pulse is negligible. While here we use latched detection only for excited-state spectroscopy, we emphasize that its usefulness is much more general.

The device [Fig. 1(a)], defined by electron-beam patterned Cr—Au depletion gates on a $GaAs/Al_{0.3}Ga_{0.7}As$ heterostructure grown by molecular-beam epitaxy, comprises two tunnel-coupled quantum dots of lithographic area 0.25 μm^2 each and two independent charge-sensing channels, one beside each central dot. The two-dimensional electron gas lies 100 nm below the surface, with bulk density 2×10^{11} cm^{-2} and mobility 2×10^{5} cm^2/V s. Each dot contains $\sim$150 electrons and has a single-particle level spacing $\Delta\sim100$ μeV (estimated from effective device area) and charging energy $E_c\sim600-700$ μeV. Left and right sensor conductances g_{ls} and g_{rs} were measured using lock-in amplifiers with 2 nA current biases at 137 and 187 Hz; double-dot conductance g_{dd} was measured using a third lock-in amplifier with a 5 μV voltage bias at 87 Hz, although during pulse-sense measurement the double dot was fully isolated and the g_{dd} and g_{rs} circuits grounded. The charge sensors were configured as QPCs by grounding gates 6, 7, 15, and 16, and were isolated from the double dot by strongly depleting gates 5, 9, 13, and 1. Measurements were carried out in a dilution refrigerator with electron temperature $\sim$100 mK.

Figure 1(b) shows the left sensor signal as a function of gate voltages V_2 and V_{10} with the device tunnel coupled to both leads. Here and in subsequent plots, a plane has been subtracted to level the central plateau to compensate for capacitive coupling between the gates and the sensor. In this regime, a honeycomb pattern characteristic of double-dot transport[6] is seen as a set of hexagonal plateaus in the left sensor conductance, with horizontally oriented steps of $\sim3\times10^{-3}e^2/h$ corresponding to changes in the number of electrons in the left dot, controlled by V_{10}, and smaller vertically oriented steps marking changes in the right dot, controlled by V_2. Steps at the short upper left and lower right segments of each hexagon reflect movement of an electron from one dot to the other, with total number fixed. Here, an increase in g_{ls} marks an electron moving *away* from the left sensor, or an increase in the number of electrons in the right dot.

Transport through the double dot, g_{dd}, occurs only at the honeycomb vertices.[8] As tunneling to the leads is reduced by making V_2 and V_{10} more negative, the honeycomb sensing pattern persists after g_{dd} has become immeasurably small, but the landscape changes dramatically as in Fig. 1(c) when the tunneling time between the double dot and the leads diverges. Here, steps follow diagonal lines of constant energy difference between the dots because only transitions from one dot to the other are allowed.

Pulse-sense measurements were carried out in this isolated configuration, with the energy difference between the dots controlled by simultaneously varying V_2 and V_{10} along diagonals [shown, for example, by the white line in Fig. 1(c)], and the interdot barrier controlled by gate voltage V_3. Fast control of the same two parameters was achieved using two synchronized Agilent 33250 arbitrary wave form generators, with rise times of $\sim$5 ns, connected to gates 11 and 12 via semirigid coaxial lines and low-temperature bias tees. To compensate a slight cross coupling of gates 11 and 12, the pulse generators produced linear combinations of pulses, denoted V_B (affecting the barrier, mainly V_{11}) and V_E (affecting the energy difference, mainly V_{12}).

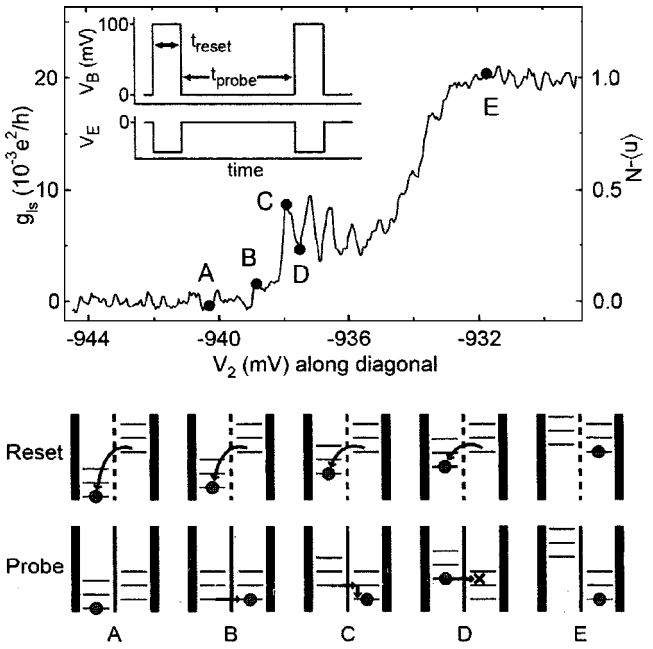

FIG. 2. Single-pulse technique. Time-averaged conductance of the left sensor as a function of V_2 along diagonal [see Fig. 1(c)] with pulses applied. Inset: Pulses on gates 11 and 12 (parametrized by V_B and V_E, controlling interdot barrier and relative energy, see text), followed by a long interval of weak tunneling. A linear fit to the left plateau is subtracted. Right axis shows the average right-dot occupation $\langle n\rangle-N$. Points $A-E$ mark features used to infer the excited-state spectrum, with schematic interpretations shown below the graph.

The single-pulse–probe sequence is shown schematically in the inset of Fig. 2. Square pulses of length $t_{reset}=100$ ns are applied every 20 μs, with $V_B=100$ mV opening the tunnel barrier while the pulse energy shift V_E is varied. The double dot relaxes to its overall ground state during the reset pulse if t_{reset} is much longer than the elastic and inelastic tunneling times τ_{el} and τ_{in} while the barrier is pulsed open, and also longer than the energy relaxation time within the dots. For the next 19.9 μs, the barrier is nearly closed, such that $\tau_{el}<t_{probe}<\tau_{in}$, and the energy levels are returned to their values before the pulse. If elastic tunneling is allowed, the electron will likely tunnel and then have ample time to relax to its ground state. If elastic tunneling is forbidden, however, the electron will likely remain where the reset pulse put it.

Figure 2 shows the sensing signal during a simultaneous ["diagonal;" see Fig. 1(c)] sweep of V_2 and V_{10}, with five

points (A to E) labeling key features. The data were taken with V_E negative, so that the pulse tilts the ground state toward the left dot. At point A, the energy difference in both the reset and probe states favors the excess charge occupying the left dot, and a flat sensing signal corresponding to a time-averaged right-dot occupation $\langle n\rangle = N$ is observed. At the opposite extreme (E), the energy difference in both cases favors the right dot, giving another flat signal $\langle n\rangle = N+1$. At point B, the ground states of the dots are degenerate in the probe state (except for small tunnel splitting). This degeneracy appears in the data as a small peak in right-dot occupation, often barely visible above the noise, presumably because tunneling in this case is reversible; the electron does not relax once it enters the right dot, so it is free to return to the left. There is a much larger peak at C. Here either an excited state in the right dot aligns with the ground state in the left or a hole excited state in the left dot aligns with the ground state in the right. After tunneling occurs the system can relax, trapping the electron in the right dot. Finally at D no excited states exist to match the initial configuration and allow elastic tunneling, so there is a dip in the right-dot occupation.

Figure 3(a) shows the sensing signal measured throughout the pulse–dc-energy-shift plane, with prominent diagonal steps marking the ground-state transitions during the pulse, and fine bands extending horizontally from each step reflecting excited-state transitions available during the probe time. Figure 3(b) presents the same data differentiated with respect to V_2 and smoothed along both axes. Here, steps in the raw signal appear as positive ridges, and excited-state peaks become bipolar. The comparison with single-dot transport spectroscopy is clear: the pulse opens an energy window, and as the window expands, more excited states become accessible and emerge from the ground-state feature. Features on the left (negative V_E) correspond to electron excited states of the right dot or hole excited states of the left; features on the right mark electron excited states of the left dot or hole excited states of the right.

Figure 3(c) shows slices of sensor conductance from Fig. 3(a) at three different V_E pulse heights, illustrating the expansion of the energy window while the positions of the emerging excited states remain fixed. The dashed curve shows the transition measured with no pulses applied. From its smooth, narrow shape, and its consistency from transition to transition, we conclude that its width is dominated by temperature broadening.[8] We associate this with a temperature of $\sim$100 mK, assuming the electron temperature in the dot is not significantly different in the tunneling regime, where it was previously calibrated.[8] This gives a lever arm $\delta V_2/\delta E = (10.5\pm1)/e$ relating changes in V_2 (along a diagonal with V_{10}) to changes in the energy of levels in the left dot relative to the right. The spacing between ground-state transitions gives the sum of the two charging energies, and assuming they are equal we find $E_c = 700\pm70$ μeV. The measured excited-state gate-voltage spacing of $\sim$0.75 mV gives an excited level spacing of $\sim$70 μeV, comparable to the $\Delta \sim 100$ μeV estimate from dot area. The slightly lower measured value may reflect sensitivity to both electron and hole excited states, giving overlapping spectra. As the energy window is increased, excited-state-to-excited-state transitions become available, further complicating the observed spectra. This may explain the blurring observed for $V_2 > -872$ mV in curve 3.

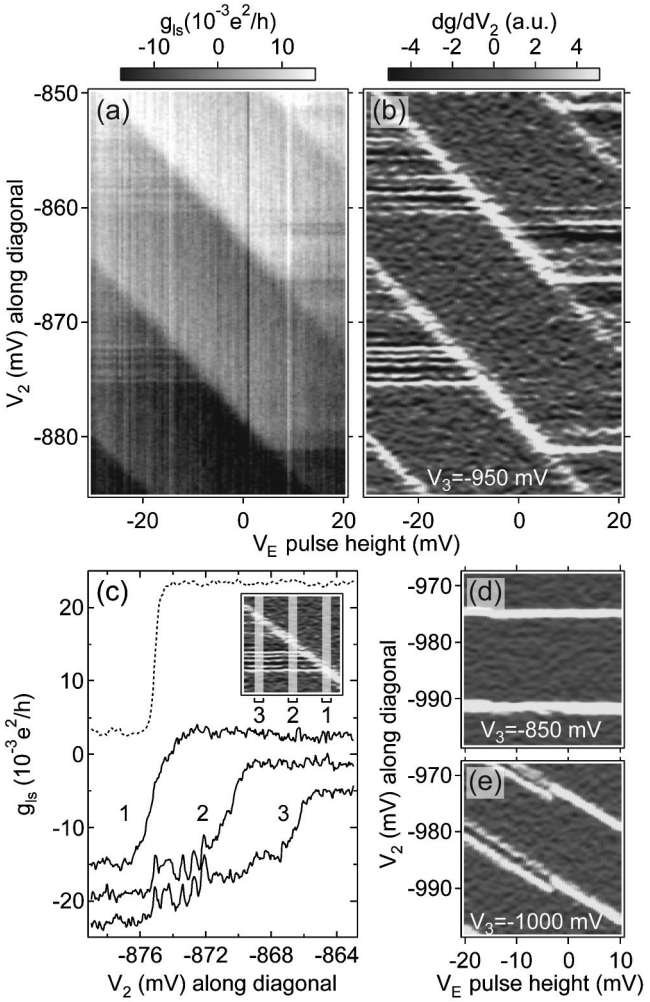

FIG. 3. (a) Left sensor conductance, and (b) its smoothed derivative with respect to V_2, as functions of V_2 and V_E. Horizontal excited state lines emerge from a diagonal ground state feature as the energy window V_E is increased. Vertical stripes in (a) result from sensor drift. (c) Slices of conductance (as in Fig. 2) as a function of V_2, averaged over different V_E ranges (see inset), offset vertically for clarity. Dashed curve is measured with pulses off. (d), (e) Sensor conductance derivative as in (b) measured with the tunnel barrier either more open (d) or more closed (e) such that the probe or the reset configuration, respectively, dominates. Color scales in (d) and (e) are the same as in (b).

Figure 3(c) shows that ground-state transitions for the pulse curves (solid) are clearly broader than for the no-pulse curve (dashed). Broadening beyond temperature is presumably due to both averaging traces with different V_E and effects of overshoot and settling of the pulse. However, as the probe step is long and insensitive to pulse properties, the excited-state peaks are not similarly broadened. In principle, the excited-state peaks are also immune to thermal broadening, their widths limited only by intrinsic decay rates, although all peaks shown here exhibit full widths at half maximum of at least $3.5kT$ (0.3 mV), possibly due to gate noise.

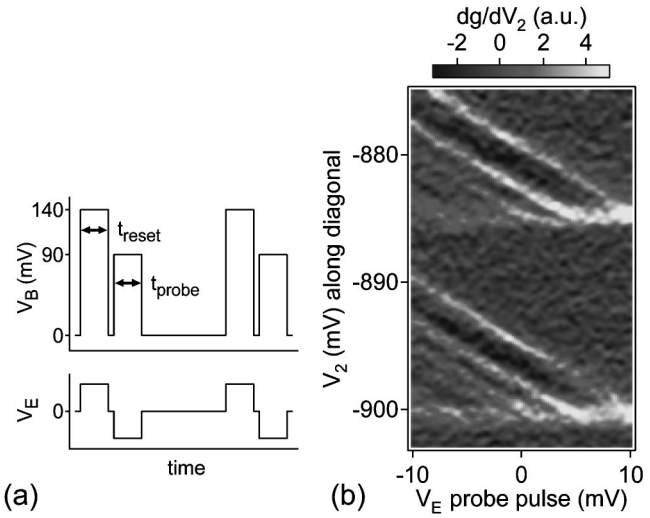

FIG. 4. (a) Two-pulse technique, shown schematically, including a reset and a probe pulse, followed by a long measurement time when no tunneling is allowed. (b) Conductance derivative with respect to V_2, shows excited states appearing now as diagonal lines.

Figures 3(d) and 3(e) repeat Fig. 3(b) with different values of gate voltage V_3, illustrating the effects of opening or closing the tunnel barrier beyond the regime of excited-state spectroscopy. Changing V_3 affects the interdot barrier both during and after the pulse, but the system is most sensitive to the tunnel rate during the probe time. Increasing tunneling by making V_3 less negative by 100 mV [Fig. 3(d)] yields single, horizontal features, as if no pulse were applied at all. This implies that $\tau_{in} \ll t_{probe}$ so the system quickly finds its ground state during the probe time regardless of relative energy levels, making the pulse irrelevant to a time-averaged measurement. Reducing tunneling by making V_3 more negative by 50 mV [Fig. 3(e)] results in diagonal features, indicating that dynamics during the pulse dominate behavior. In the right half of this plot there is a single transition, implying that the system finds its ground state while the pulse is on; then the barrier is closed such that $\tau_{el}, \tau_{in} \gg t_{probe}$ and no further tunneling is permitted. On the left there are two diagonal features, implying that an excited state is populated at the start of the reset pulse. This effect is not understood at present, nor is it specific to the too-closed-barrier regime; it is occasionally seen along with the understood horizontal excited-state features.

We now turn to the second pulse-sense method described above, latched detection, using two pulses on each gate as shown in Fig. 4(a). Figure 4(b) shows the derivative of the sensor signal measured in this configuration as a function of V_2 and the V_E probe pulse height, using $t_{reset}=t_{probe}=20$ ns, $V_{B,reset}=140$ mV, and $V_{B,probe}=90$ mV. Here we vary the probe properties rather than the reset properties as in Fig. 3, so excited states appear diagonally and the reset ground state is horizontal. Excited states measured this way are not immune to pulse properties, and as a result, the data in Fig. 4 are blurred relative to Fig. 3. This diminished resolution is not fundamental, and can be reduced with more accurate pulse shaping.

We thank M. J. Biercuk and A. Yacoby for useful discussions and K. Crockett for experimental contributions. This work was supported in part by DARPA QuIST, Harvard NSF-NSEC, and iQuest at UCSB.

[1] J. A. Folk, C. M. Marcus, and J. S. Harris, Jr., Phys. Rev. Lett. **87**, 206802 (2001); I. L. Aleiner, P. W. Brouwer, and L. I. Glazman, Phys. Rep. **358**, 309 (2002).

[2] D. Loss and D. P. DiVincenzo, Phys. Rev. A **57**, 120 (1998); D. D. Awschalom, D. Loss, and N. Samarth, *Semiconductor Spintronics and Quantum Computation* (Springer, Berlin, 2002).

[3] S. A. Gurvitz, Phys. Rev. B **56**, 15 215 (1997); E. Buks *et al.*, Nature (London) **391**, 871 (1998); A. N. Korotkov and D. V. Averin, Phys. Rev. B **64**, 165310 (2001); S. Pilgram and M. Buttiker, Phys. Rev. Lett. **89**, 200401 (2002); U. Hartmann, and F. K. Wilhelm, Phys. Status Solidi B **233**, 385 (2002).

[4] A. T. Johnson *et al.*, Phys. Rev. Lett. **69**, 1592 (1992); D. R. Stewart *et al.*, Science **278**, 1784 (1997).

[5] N. C. van der Vaart *et al.*, Phys. Rev. Lett. **74**, 4702 (1995); U. Sivan *et al.*, Europhys. Lett. **25**, 605 (1994).

[6] W. G. van der Wiel *et al.*, Rev. Mod. Phys. **75**, 1 (2003).

[7] M. Field *et al.*, Phys. Rev. Lett. **70**, 1311 (1993); I. Amlani *et al.*, Appl. Phys. Lett. **71**, 1730 (1997); D. S. Duncan *et al.*, *ibid.* **74**, 1045 (1999); J. M. Elzerman *et al.*, Phys. Rev. B **67**, 161308 (2003).

[8] L. Dicarlo *et al.*, Phys. Rev. Lett. **92**, 226801 (2004).

[9] T. Fujisawa *et al.*, J. Phys.: Condens. Matter **15**, R1395 (2003).

[10] J. M. Elzerman *et al.*, Appl. Phys. Lett. **84**, 4617 (2004).